



Effects of Diabetes Mellitus on the Disposition of Tofacitinib, a Janus Kinase Inhibitor, in Rats

Eun Hye Gwak, Hee Young Yoo and So Hee Kim*

College of Pharmacy and Research Institute of Pharmaceutical Science and Technology, Ajou University, Suwon 16499, Republic of Korea

Abstract

Tofacitinib, a Janus kinase inhibitor, was developed for the treatment of rheumatoid arthritis. Recently, it has been associated with an increased change in arthritis development in patients with diabetes. Herein, we evaluated the pharmacokinetics of tofacitinib after intravenous (10 mg/kg) and oral (20 mg/kg) administration to rats with streptozotocin-induced diabetes mellitus and control rats. Following intravenous administration of tofacitinib to rats with streptozotocin-induced diabetes mellitus, area under the plasma concentration-time curve from time zero to infinity of tofacitinib was significantly smaller (33.6%) than that of control rats. This might be due to the faster hepatic intrinsic clearance (112%) caused by an increase in the hepatic cytochrome P450 (CYP) 3A1(23) and the faster hepatic blood flow rate in rats with streptozotocin-induced diabetes mellitus than in control rats. Following oral administration, area under the plasma concentration-time curve from time zero to infinity of tofacitinib was also significantly smaller (55.5%) in rats with streptozotocin-induced diabetes mellitus than that in control rats. This might be due to decreased absorption caused by the higher expression of P-glycoprotein and the faster intestinal metabolism caused by the higher expression of intestinal CYP3A1(23), which resulted in the decreased bioavailability of tofacitinib (33.0%) in rats with streptozotocin-induced diabetes mellitus. In summary, our findings indicate that diabetes mellitus affects the absorption and metabolism of tofacitinib, causing faster metabolism and decreased intestinal absorption in rats with streptozotocin-induced diabetes mellitus.

Key Words: Tofacitinib, CYP3A1(23), Streptozotocin-induced diabetes mellitus, P-pg, Intrinsic clearance, Pharmacokinetics

INTRODUCTION

Tofacitinib, [3-[(3R,4R)-4-methyl-3-[methyl-(7H-pyrrolo[2,3-d]pyrimidin-4-yl)amino]piperidin-1-yl]-3-oxopropanenitrile] (Fig. 1), a novel Janus kinase (JAK) 1 and 3 inhibitor (Coombs *et al.*, 2010; Gupta *et al.*, 2012), was developed for the treatment of rheumatoid arthritis. Tofacitinib blocks several cytokine receptors for interleukin-2, -4, -7, -9, -15, and -21 by inhibiting JAK 1 and 3, and modulates multiple immune responses (LaBranchem *et al.*, 2012). Tofacitinib was thus approved to treat rheumatoid arthritis, particularly in patients that are intolerant to methotrexate therapy (Claxton *et al.*, 2018). Tofacitinib was also approved for the treatment of moderate to severe ulcerative colitis in 2018 (Fukuda *et al.*, 2019) and was the first oral JAK inhibitor approved for chronic use by ulcerative colitis patients (Antonelli *et al.*, 2018). Furthermore, tofacitinib is currently being evaluated in the clinic for various diseases, such as psoriasis (Bachelez *et al.*, 2015; Papp *et al.*, 2015), alopecia (Kennedy Crispin *et al.*, 2016), atopic dermatitis (Levy *et*

al., 2015), and ankylosing spondylitis (Tahir, 2018).

Tofacitinib is rapidly absorbed and eliminated and has a terminal half-life of approximately 3.3 h (Lawendy *et al.*, 2009; Dowty *et al.*, 2014). Tofacitinib is primarily metabolized via cytochrome P450 (CYP) 3A4 followed by CYP2C19 in humans (Gupta *et al.*, 2012; Dowty *et al.*, 2014); thus, approximately 70% is eliminated non-renal, while 30% is excreted renally in humans (Lawendy *et al.*, 2009; Dowty *et al.*, 2014). Tofacitinib is known as a substrate of P-glycoprotein (P-gp) (Hussa, 2014). The pharmacokinetics of tofacitinib was investigated in patients with a variety of diseases, including rheumatoid arthritis (Riese *et al.*, 2010), psoriasis (Ma *et al.*, 2018), and renal transplant recipients (Vincenti *et al.*, 2012). However, its pharmacokinetic changes under diabetic conditions is not well known. One of the most frequent diseases in patients with diabetes is osteoporotic arthritis, but the association between diabetes and rheumatoid arthritis has been increasing because of the accompanied chronic inflammation, which is similar to that in osteoporotic arthritis (Molsted *et al.*, 2018).

Open Access <https://doi.org/10.4062/biomolther.2020.006>

This is an Open Access article distributed under the terms of the Creative Commons Attribution Non-Commercial License (<http://creativecommons.org/licenses/by-nc/4.0/>) which permits unrestricted non-commercial use, distribution, and reproduction in any medium, provided the original work is properly cited.

Received Jan 16, 2020 Revised Feb 14, 2020 Accepted Feb 21, 2020
Published Online Mar 25, 2020

*Corresponding Author

E-mail: shkim67@ajou.ac.kr

Tel: +82-31-219-3451, Fax: +82-31-219-3435

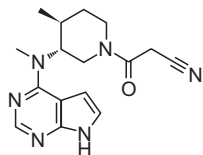


Fig. 1. Structure of tofacitinib.

A diabetic animal model can be established using diabetogenic chemicals, such as alloxan, streptozotocin, and the zinc chelator (Pickup and Williams, 1991; Watkins and Sandeors, 1995). Streptozotocin induces structural changes in pancreatic beta cells within 48 h after intravenous or intraperitoneal administration, causing the diabetic status to maintain for 4 months (Watkins and Sandeors, 1995). Moreover, the diabetic condition induced by streptozotocin caused a decrease in bile flow rate and changes in bile compositions (Carnovale *et al.*, 1986), impaired kidney function (Nadai *et al.*, 1990; Park *et al.*, 1996), and hepatotoxicity (Watkins and Sherman, 1992). Streptozotocin-induced diabetes mellitus (SIDM) profoundly affects the disposition of drugs, especially absorption and metabolism, due to the alteration in the expression of CYP isoforms (major drug metabolizing enzymes) and P-gp (a major efflux transporter) in the liver and intestine. Although the relationship between the expression of CYP isoforms and P-gp has not been reported, alterations of CYP isoforms and P-gp expression induced by diabetes might play a role in the disposition of drugs. The expression and activity of hepatic CYP isoforms in diabetes mellitus was assessed using different diabetic rat models (Lee *et al.*, 2010). However, adequate evaluation of the changes in CYP isoforms and P-gp expression in the intestine of diabetes mellitus rats have not been performed.

In the present study, we investigated the effects of diabetes mellitus on the disposition of tofacitinib using an SIDM rat model after intravenous and oral administration of 10 and 20 mg/kg of the drug, respectively. Alterations in activities and protein expression of the CYP isoforms in the hepatic and intestinal microsomal proteins were also evaluated.

MATERIALS AND METHODS

Chemicals

Tofacitinib citrate, streptozotocin, and hydrocortisone, the internal standard for high-performance liquid chromatography (HPLC) analysis, were obtained from Sigma-Aldrich (St. Louis, MO, USA). Heparin and 0.9% NaCl-injectable solution were purchased from JW Pharmaceutical Corporation (Seoul, Korea). Ethyl acetate, methanol and acetonitrile was procured from J.T. Baker (Phillipsburg, NJ, USA), and β -cyclodextrin was obtained from Wako (Osaka, Japan). The primary antibodies against CYP1A1/2, CYP2B1/2, CYP2C11, CYP2D6, CYP2E1, and CYP3A1(23) were purchased from Detroit R & D Inc (Detroit, MI, USA). P-gp and glyceraldehyde 3-phosphate dehydrogenase (GAPDH) were obtained from Cell Signaling Technology (Beverly, MA, USA) and Sigma-Aldrich, respectively. Secondary rabbit and mouse antibodies were products of Bio-Rad (Hercules, CA, USA). All other chemicals were of HPLC-grade and were used without further purification.

Animals

Male Sprague-Dawley rats (age, 7-8 weeks and weight, 240-260 g) were purchased from OrientBio Korea (Seongnam, Korea), housed in a clean room under condition of a temperature of $22 \pm 1^\circ\text{C}$, relative humidity of $50 \pm 5\%$ and 12-h light (7:00-19:00) and 12-h dark (19:00-7:00) cycles with air filtration (Laboratory Animal Research Center of Ajou University Medical Center, Suwon, Korea). Rats had access to food and water *ad libitum*. All experimental procedures and protocols were reviewed and approved by the Institutional Animal Care and Use Committee (IACUC No. 2014-0053) of the Laboratory Animal Research Center of Ajou University Medical Center.

Induction of diabetes mellitus

Diabetes mellitus was induced in rats by a single intraperitoneal injection of streptozotocin (60 mg/kg, dissolved in 10 mM sodium citrate buffer, pH 4.5), while the control group was injected with 10 mM sodium citrate buffer only (Choi *et al.*, 2008). Rats were fasted overnight with free access to water. Blood sugar levels were measured in rats on 7th day after injecting streptozotocin or 10 mM sodium citrate buffer using a glucose detection kit (Caresens, Seoul, Korea). Rats with a blood glucose level higher than 250 mg/dL were selected for the study (Choi *et al.*, 2008).

Preliminary study

For the preliminary study, plasma samples were collected from SIDM and control rats ($n=3$, each group). Subsequently, albumin, total protein, urea nitrogen, glutamate oxaloacetate transaminase (GOT), glutamate pyruvate transaminase (GPT), and creatinine levels were measured (Green Cross Reference Lab, Seoul, Korea). Urine samples were collected for 24 h and the exact urine volume and creatinine levels were also measured. Whole liver and kidney of each rat were then excised and weighed.

Intravenous and oral administration of tofacitinib

The pretreatment and surgical procedures for intravenous and oral administration were similar to those described previously (Kim *et al.*, 1993; Lee and Kim, 2019). For oral administration, rats were fasted overnight with free access to water. Rats were then anesthetized with ketamine (100 mg/kg), and their carotid arteries and jugular veins (intravenous only) were cannulated using polyethylene tubing (Clay Adams, Parsippany, NJ, USA) for blood sampling and drug administration, respectively.

For intravenous administration, tofacitinib, dissolved in 0.9% NaCl-injectable solution containing 0.5% β -cyclodextrin, was injected via the jugular vein for 1 min at a dose of 10 mg/kg to control ($n=9$) and SIDM ($n=7$) rats. Blood samples (110 μL) were collected via the carotid artery at times 0 (prior to drug administration), 1 (at the end of drug infusion), 5, 15, 30, 45, 60, 90, 120, 180, 240, 360, 480, and 600 min, and immediately centrifuged at 8,000 g for 10 min and plasma was collected. Urine samples were collected over 24 h. In addition, each metabolic cage was rinsed with 20 mL of distilled water 24 h after drug administration, and the rinses were combined with their corresponding 24-h urine samples. The volumes of the combined urine samples were measured and two 50- μL aliquots of each were collected. At 24 h, the abdomen of each rat was opened and the entire gastrointestinal tract, including its contents and feces, was removed, transferred to a bea-

ker containing 50 mL methanol, cut into small pieces, stirred manually, and two 50- μ L aliquots of each supernatant were collected. All samples collected above were stored at -80°C until HPLC analysis of tofacitinib (Lee and Kim, 2019).

For oral administration, approximately 1 mL of 20 mg/kg tofacitinib was administered to control (n=8) and SIDM (n=7) rats. Blood samples (110 μ L) were collected via the carotid artery at times 0 (prior to drug administration), 5, 15, 30, 45, 60, 90, 120, 180, 240, 360, 480, 600, and 720 min. Urine and gastrointestinal tract samples were obtained over 24 h and were processed similarly using the above procedure.

Tissue distribution of tofacitinib

Rats were handled and processed as described previously (Lee and Kim, 2019). Tofacitinib (10 mg/kg) was intravenously administered to control and SIDM rats (n=3, each group). After 30 min, the maximum attainable blood was collected from the carotid artery. Blood samples were immediately centrifuged and plasma was collected. Rats were sacrificed by cervical dislocation. Thereafter, approximately 1 g of each brain, fat, heart, kidney, large intestine, liver, lung, mesentery, muscle, small intestine, spleen, and stomach was removed, rinsed with phosphate-buffered solution (pH 7.4), and blotted dry with paper towels to remove any remaining blood. Each tissue sample was added to 4 volumes of homogenizing buffer, homogenized using a tissue homogenizer (T25 Ultra-Turrax, IKA Labortechnik, Staufen, Germany) and centrifuged at 8,000 g for 10 min. A 50- μ L aliquot of each supernatant was collected and stored at -80°C until HPLC analysis of tofacitinib (Lee and Kim, 2019).

Measurement of V_{\max} , K_m , and CL_{int}

The procedures used for the preparation of hepatic and intestinal microsomes were similar to a previously reported method (Choi *et al.*, 2008). Protein contents in hepatic and intestinal microsomes were measured using a BCA assay. The maximum velocity (V_{\max}) and apparent Michaelis–Menten constant (K_m ; the concentration at which the rate is one-half of V_{\max}) for the disappearance of tofacitinib were determined after the above microsomes (equivalent to 1 mg proteins) were incubated with 5 μ L of dimethylsulfoxide containing final tofacitinib concentrations of 1, 1.5, 2, 3.5, 5, 10, 50, 100, 200 and 300 μ M, and NADPH generating system. The volume was adjusted to 1 mL by adding 0.1 M phosphate buffer (pH 7.4), and the components were incubated in a water-bath shaker maintained at 37°C and 50 oscillations per min (opm) for 15 min. The above microsomal incubation conditions were in the linear range of the reaction rate. After incubation, the reaction was terminated by adding 2 volumes of acetonitrile. Thereafter, two 50- μ L aliquots of the reaction mixture were collected. The kinetic constants (K_m and V_{\max}) for the disappearance of tofacitinib were calculated using a Lineweaver-Burk plot (Dugleby, 1995; Choi *et al.*, 2008). The intrinsic clearance (CL_{int}) for the disappearance of tofacitinib was calculated by dividing the V_{\max} by the K_m .

Immunoblot analysis

For immunoblot analysis, the hepatic and intestinal microsome protein samples (20–40 μ g protein per lane) were resolved via sodium dodecyl sulfate polyacrylamide gel electrophoresis (SDS-PAGE) on a gel (10%) and transferred to nitrocellulose for 1 h. For immunodetection, blots were incu-

bated overnight with the appropriate diluted primary antibody (1:1,000) in 5% bovine serum albumin (BSA) and tris-buffered saline (TBS) with 0.1% tween 20 (TBS-T) at 4°C with gentle shaking; this was followed by incubation with a secondary antibody conjugated to horseradish peroxidase for 1 h at room temperature. Protein expression level was detected via enhanced chemiluminescence (Detroit R & D Inc.) using an ImageQuant LAS-4000 mini (GE Healthcare Life Sciences, Piscataway, NJ, USA). Band density was quantified using ImageJ 1.45s software (NIH, Bethesda, MD, USA). GAPDH was used as an internal standard (Bae *et al.*, 2018).

Rat plasma protein binding study of tofacitinib

The values for protein binding of tofacitinib to fresh plasma from control and SIDM rats (n=3, each group) were determined using equilibrium dialysis (Kim *et al.*, 1999). Briefly, 1 mL of rat plasma from control or SIDM rats was dialyzed against the same volume of isotonic Sørensen phosphate buffer (pH 7.4) containing 3% dextran (“the buffer”) to minimize volume shift (Shin *et al.*, 1991; Kim *et al.*, 1999) using a dialysis cell (Spectrum Medical Industries, Los Angeles, CA, USA) and a Spectra/Por 2 membrane (molecular weight cut-off 12,000–14,000 Da; Spectrum Medical Industries). To minimize the time to reach equilibrium, 10 μ g/mL tofacitinib was spiked in the plasma compartment (Svein and Theodor, 1982; Shin *et al.*, 1991). After the dialyzed cells were incubated at a rate of 50 opm in a water-bath shaker at 37°C for 24 h, a 50- μ L aliquot was withdrawn from each compartment, and the concentrations of tofacitinib in the buffer (C_B) and rat plasma (C_P) compartments were measured. Percent binding (%) was calculated as:

$$\% = \frac{C_P - C_B}{C_P} \times 100$$

HPLC analysis

One microliters of hydrocortisone (internal standard, 5 mg/mL) and 20 μ L of 20% ammonia solution were added to 50- μ L aliquots of biological samples and mixed for 30 s with a vortex mixer. Each solution was extracted with 750 μ L of ethyl acetate by centrifugation at 12,000 rpm for 5 min. The organic layer was collected and dried on a dry thermobath (Eyela, Tokyo, Japan) under a gentle stream of nitrogen gas at 40°C . The samples were reconstituted in 130 μ L of 20% acetonitrile, and 50 μ L of resuspended samples were analyzed by HPLC (Lee and Kim, 2019).

The concentrations of tofacitinib in the prepared biological samples were determined using a Prominence LC-20A HPLC system (Shimadzu, Kyoto, Japan), consisting of a pump (LC-20A), an auto-sampler (SIL-20A), a column oven, and a detector (SPD-20A/20AD), controlled with a CBM-20A system controller. The samples were filtered and separated on a reversed-phase column (C_{18} ; 25 cm \times 4.6 mm, 5 μ m; Young Jin Biochrom, Seongnam, Korea). The mobile phase consisted of 10 mM ammonium acetate buffer (pH 5.0) and acetonitrile in a 69.5:30.5 (v/v) ratio. Flow rate was 1.0 mL/min. Column effluent was monitored by a UV detector at 287 nm. The retention times of tofacitinib and the internal standard were approximately 7.21 and 11.3 min, respectively. The lower limits of quantitation of tofacitinib in rat plasma, urine, and tissue homogenates were 0.01, 0.1, and 0.1 μ g/mL, respectively, with intraday assay precision (coefficients of variation) of 3.69–

5.88%, 4.21-6.18%, and 1.11-8.74%, respectively. The inter-day assay precision was 5.06% for rat plasma and 5.46% for rat urine.

Pharmacokinetic analysis

Pharmacokinetic parameters, including the area under the plasma concentration-time curve from time zero to infinity (AUC), apparent volume of distribution at steady state (V_{ss}), mean residence time (MRT), time-averaged total body (CL), renal (CL_R) and nonrenal (CL_{NR}) clearances were calculated by noncompartmental analysis (WinNonlin, Pharsight Corporation, Mountain View, CA, USA) using standard methods (Gibaldi and Perrier, 1982). The AUC values were calculated using the trapezoidal rule–extrapolation method (Chiou, 1978), while peak plasma concentration (C_{max}) and time to reach C_{max} (T_{max}) were obtained directly from the experimental data.

The glomerular filtration rate (GFR) was estimated by calculating creatinine clearance (CL_{CR}), with the assumption that kidney function was stable during the experimental period. The CLCR was calculated by dividing the total amount of unchanged creatinine excreted in the urine over 24 h by the $AUC_{0-24 h}$ of creatinine in plasma.

Statistical analysis

The results are expressed as mean \pm standard deviation (SD), except that of T_{max} , which was expressed as median (range). Comparisons between 2 means were carried out using Student’s unpaired *t*-tests. A *p* value <0.05 was considered statistically significant.

RESULTS

Preliminary study

Blood glucose level, plasma chemistry data, CL_{CR} , and oth-

Table 1. Body weight, urine output, plasma chemistry data and relative organs weight in control and streptozotocin-induced diabetes mellitus (SIDM) rats

Parameters	Control (n=3)	SIDM (n=3)
Body weight (g)		
Initial	267 \pm 8.77	271 \pm 6.31
Final	281 \pm 19.6	243 \pm 13.6***
Blood glucose (mg/dL)	151 \pm 19.5	444 \pm 117***
Urine output (mL/kg/24 h)	110 \pm 22.6	136 \pm 24.7*
Plasma		
Total protein (g/dL)	5.80 \pm 0.379	5.53 \pm 0.231
Albumin (g/dL)	3.90 \pm 0.30	3.73 \pm 0.153
Urea nitrogen (mg/dL)	16.3 \pm 3.21	35.0 \pm 2.00***
GOT (IU/L)	59.3 \pm 5.77	95.3 \pm 21.4*
GPT (IU/L)	35.0 \pm 6.24	68.0 \pm 11.9**
S_{CR} (mg/dL)	0.778 \pm 0.102	1.40 \pm 0.173
CL_{CR} (mL/min/kg)	2.50 \pm 0.232	1.53 \pm 0.390*
Plasma protein binding (%)	23.1 \pm 1.82	21.9 \pm 1.21
Liver weight (% of body weight)	3.67 \pm 0.623	3.72 \pm 0.640
Kidney weight (% of body weight)	0.803 \pm 0.185	1.07 \pm 0.088**

CL_{CR} , creatinine clearance; GOT, glutamate oxaloacetate transaminase; GPT, glutamate pyruvate transaminase; SCR , serum creatinine concentration. **p*<0.05, ***p*<0.01, ****p*<0.001.

er related physiological data in control and SIDM rats are summarized in Table 1. Compared to control rats, plasma levels of GOT and GPT were significantly higher by 60.7% and 94.3%, respectively, in SIDM rats. The values in SIDM rats were also higher than the reported normal ranges for rats (i.e., 45.7 and 17.5 IU/L for GOT and GPT, respectively (Mitruka and Rawnsley, 1981). The relative weight of the liver did not significantly differ between the 2 groups and no histological changes were observed in the liver of both control and SIDM rats. These findings suggest that the hepatic function was not severely impaired in SIDM rats compared to control rats. The plasma level of urea nitrogen was significantly higher (by 115%) and relative weight of the kidney was significantly greater (33.3% increase) in SIDM rats than control rats. In addition, serum creatinine (S_{CR}) level was significantly greater by 79.9%, while CL_{CR} was significantly slower by 38.8% in SIDM rats relative to control rats. There were no significant changes in the kidney histology of both groups. Such findings suggest that kidney function was impaired in SIDM rats. The plasma levels of total proteins and albumin did not significantly differ between the 2 groups; these values were similar to the reported ranges in normal rats (Mitruka and Rawnsley, 1981).

Pharmacokinetics of tofacitinib after intravenous and oral administration

Fig. 2A displays the mean arterial plasma concentration–time profiles of tofacitinib after the intravenous administration of 10 mg/kg to control and SIDM rats. Their relevant pharmacokinetic parameters are summarized in Table 2. Compared to control rats, SIDM rats had lower mean arterial plasma concentration of tofacitinib; thus, SIDM rats had significantly smaller AUC values (by 33.6%) than control rats. CL , CL_R , and CL_{NR} were significantly higher (by 51.1%, 87.5%, and 43.8%, respectively) in SIDM rats than those in control rats. Further, V_{ss} value was significantly greater (by 262%) in SIDM rats than that in control rats, but the percentage of the dose excreted in urine for 24 h ($Ae_{0-24 h}$) and terminal half-life of tofacitinib remained unchanged in the 2 groups. The remaining percentage of the tofacitinib dose in the gastrointestinal tract (including its contents and feces) at 24 h ($GI_{24 h}$) was low (the values were 0.0935% and 0.282% in control and SIDM rats, respectively).

Fig. 2B displays the mean arterial plasma concentration–time profiles of tofacitinib after the oral administration of 20 mg/kg to control and SIDM rats. Some of the relevant pharmacokinetic parameters of tofacitinib are summarized in Table

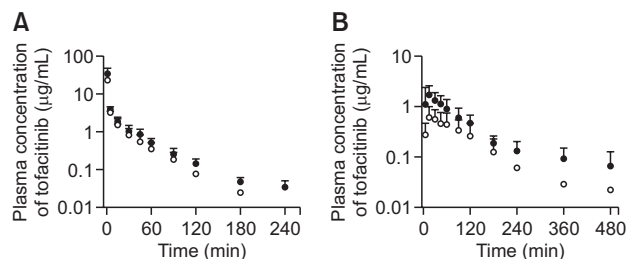


Fig. 2. Mean arterial plasma concentration–time profiles of tofacitinib after a 1-min intravenous infusion of tofacitinib (10 mg/kg) to control (●; n=9), and streptozotocin-induced diabetes mellitus (SIDM) (○; n=7) rats (A) and oral administration of tofacitinib (20 mg/kg) to control (●; n=8) and SIDM (○; n=7) rats (B). Vertical bars represent standard deviation.

Table 2. Pharmacokinetic parameter of tofacitinib after intravenous (10 mg/kg) and oral (20 mg/kg) administration to control and streptozotocin-induced diabetes mellitus (SIDM) rats

Parameter	Intravenous		Oral	
	Control (n=9)	SIDM (n=)	Control (n=8)	SIDM (n=)
Body weight (g)	290 ± 17.2	245 ± 13.0 ^{***}	269 ± 16.2	241 ± 15.9 ^{**}
Blood glucose (mg/dL)	158 ± 17.4	499 ± 87.2 ^{***}	142 ± 19.9	395 ± 124 ^{***}
AUC (μg·min/mL)	256 ± 37.3	170 ± 29.4 ^{**}	182 ± 26.4	81 ± 42.9 ^{***}
C _{max} (μg/mL)			1.75 ± 1.07	0.68 ± 0.36 [*]
T _{max} (min)			17.9 ± 9.1	25.7 ± 16.7
Terminal half-life ₂ (min)	30.2 ± 4.83	26.5 ± 2.81		
MRT (min)	21.3 ± 9.28	44.3 ± 19.5 [*]		
CL (mL/min/kg)	39.9 ± 6.74	60.3 ± 11.1 ^{**}		
CL _R (mL/min/kg)	2.56 ± 0.59	4.80 ± 1.57 ^{**}	8.86 ± 13.5	21.7 ± 14.9 [*]
CL _{NR} (mL/min/kg)	38.6 ± 8.04	55.5 ± 9.79 ^{**}		
V _{SS} (mL/kg)	986 ± 379	3565 ± 2379 ^{**}		
GI _{24h} (% of dose)	0.0935 ± 0.0367	0.282 ± 0.173	0.177 ± 0.123	0.238 ± 0.160
Ae _{0-24h} (% of dose)	6.99 ± 2.30	6.64 ± 1.65	7.98 ± 1.34	6.94 ± 2.42
F (%)			35.5	23.8

Ae_{0-24h}, the percentage of the dose excreted in urine for 24 h; AUC, area under the plasma concentration-time curve from time zero to infinity; C_{max}, maximum plasma concentration; CL, time-averaged total body clearance; CL_{NR}, time-averaged non-renal clearance; CL_R, time-averaged renal clearance; F, bioavailability; GI_{24h}, the percentage of the dose remaining in the gastrointestinal tract at 24 h; MRT, mean residence time; T_{max}, time to reach C_{max}; V_{SS}, volume of distribution of steady state. **p*<0.05, ***p*<0.01, ****p*<0.001.

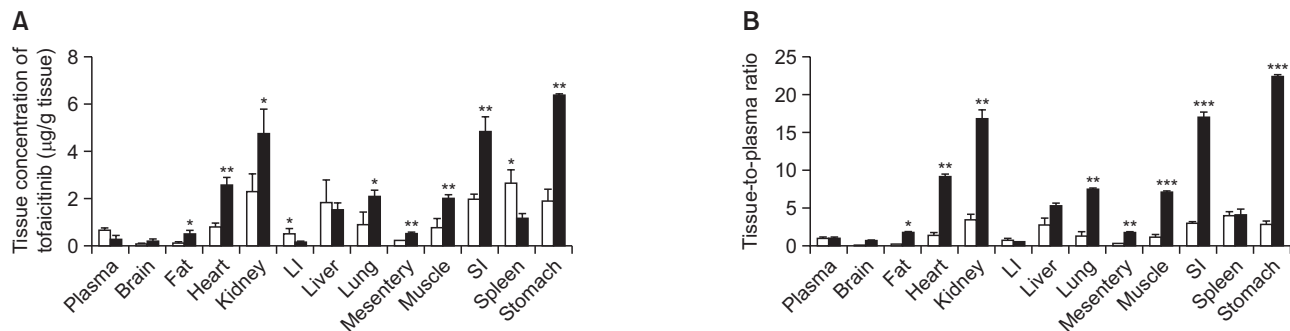


Fig. 3. Mean tissue concentration (μg/g tissue) (A) and the tissue to plasma (T/P) ratios (B) of tofacitinib 30 min after a 1-min intravenous infusion of 10 mg/kg to control (white) and streptozotocin-induced diabetes mellitus (SIDM, black) rats (n=3, each group). Vertical bars represent standard deviation. LI, large intestine; SI, small intestine. **p*<0.05, ***p*<0.01, ****p*<0.001.

2. The absorption of tofacitinib in the gastrointestinal tract was rapid; tofacitinib was detected in the plasma at the first blood sampling time point (5 min) in all rats. Compared to control rats, SIDM rats had lower mean arterial plasma concentration; the AUC and C_{max} values were significantly lower (by 55.5% and 61.1%, respectively) in SIDM rats than those in control rats. The CL_R value was significantly higher (by 145%) in SIDM rats than that in control rats, owing to the relatively smaller AUC values in SIDM rats. The GI_{24h} of tofacitinib remained unchanged in the 2 groups, with values of 0.177% and 0.238% when the oral dose was administered to the control and SIDM rats, respectively. Such findings indicate that the gastrointestinal absorption of tofacitinib was almost complete in both groups. The bioavailability (F) values of tofacitinib after oral administration were 35.5% and 23.8% for control and SIDM rats, respectively.

Tissue distribution of tofacitinib

Each tissue concentration (μg/mL for plasma or μg/g for tissue) and the tissue-to-plasma (T/P) ratios of tofacitinib at 30 min after intravenous administration of 10 mg/kg are shown in Fig. 3. Tofacitinib was widely distributed in both groups. Although the plasma concentration of tofacitinib was lower in SIDM rats than control rats, the tissue concentration of tofacitinib was generally higher in SIDM rats than control rats. The concentrations and T/P ratios of tofacitinib were significantly higher in the fat, heart, kidney, lung, mesentery, muscle, small intestine, and stomach of SIDM rats than control rats.

In vitro metabolism of tofacitinib in the hepatic and intestinal microsomes

The V_{max}, K_m, and CL_{int} values for the disappearance of tofacitinib in the hepatic and intestinal microsomes from both groups are shown in Fig. 4. The K_m values in the hepatic microsomes from SIDM rats were significantly smaller (by

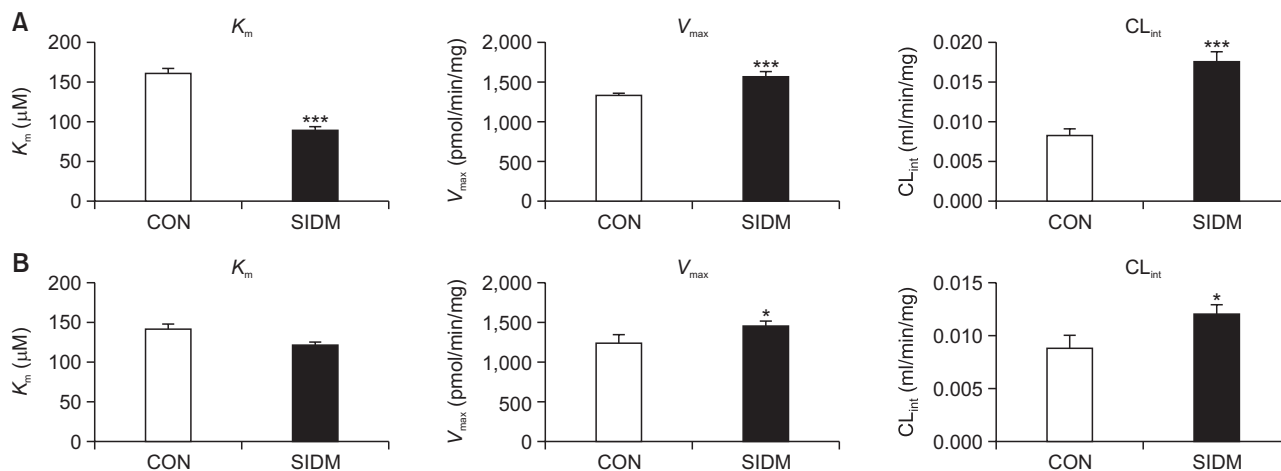


Fig. 4. Measurement of K_m , V_{max} , and CL_{int} for the disappearance of tofacitinib in hepatic (A) and intestinal (B) microsomes prepared from control (CON) and streptozotocin-induced diabetes mellitus (SIDM) rats (n=3, each group). This experiment was performed 3 times and data are expressed as mean \pm standard deviation (n=3). K_m , Michaelis-Menten constant; V_{max} , maximum velocity; CL_{int} , intrinsic clearance. * p <0.05, *** p <0.001.

44.3%, p <0.001) in SIDM rats than those in control rats. The V_{max} and CL_{int} values were significantly faster by 18.4% and 112%, respectively, in SIDM rats than those in control rats, suggesting that the *in vitro* metabolism of tofacitinib was affected by diabetes mellitus in the rat liver. However, K_m values for tofacitinib in the intestinal microsome were comparable between the 2 groups, but V_{max} and CL_{int} values were significantly faster by 16.9% and 35.4%, respectively, in SIDM rats than those in control rats, suggesting that the *in vitro* metabolism of tofacitinib was also affected by diabetes mellitus in the rat intestine.

Protein expression of the CYP isoforms and P-gp

The protein expression of CYP1A1/2, CYP2B1/2, CYP2E1, CYP2D6, and CYP3A1(23) were remarkably increased, while CYP2C11 was decreased in the hepatic microsome of SIDM rats (Fig. 5A). Similarly, the protein expression of CYP2B1/2, CYP2E1, CYP2D6, and CYP3A1(23) were also increased in the intestinal microsome of SIDM rats, while the intestinal expression of CYP1A1/2 and CYP2C11 were either comparable or slightly decreased in SIDM rats (Fig. 5B). The expression level of P-gp was decreased in the hepatic microsome of SIDM rats but markedly increased in the intestinal microsome of SIDM rats. These findings suggest that diabetes mellitus affected the protein expression of CYP enzymes and P-gp, and might result in changes in the absorption and metabolism of tofacitinib.

Rat plasma protein binding of tofacitinib

The values for protein binding of tofacitinib to the fresh plasma from control and SIDM rats were $23.1 \pm 1.82\%$ and $21.9 \pm 1.21\%$, respectively (Table 1). We found no significant differences between the protein binding values of the 2 groups. Lee and Kim (2019) reported that the binding of tofacitinib to 4% human serum albumin, similar to the ratio of albumin in rat plasma (Mitruka and Rawnsley, 1981), was independent of the tofacitinib concentration ranging from 1 to 100 $\mu\text{g/mL}$; the mean value was $22.5 \pm 1.52\%$. Thus, tofacitinib concentration of 10 $\mu\text{g/mL}$ was selected for the plasma protein binding study.

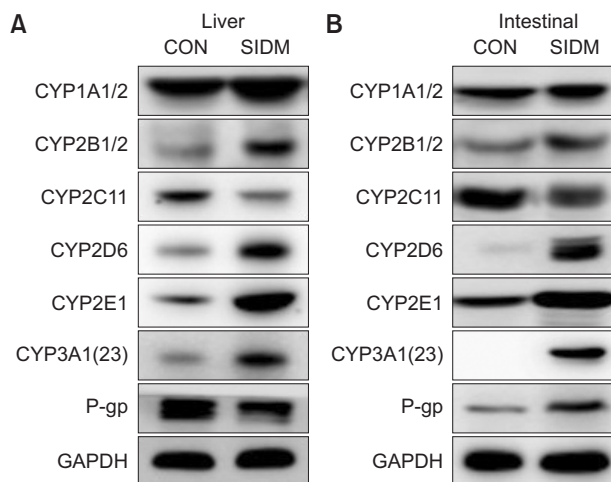


Fig. 5. Protein expression of the cytochrome P450 (CYP) isoforms and P-glycoprotein (P-gp) in hepatic (A) and intestinal (B) microsomes prepared from control (CON) and streptozotocin-induced diabetes mellitus (SIDM) rats by immunoblot analyses. Glyceraldehyde 3-phosphate dehydrogenase (GAPDH) was used as the loading control. This experiment was performed 3 times. Band density was estimated using ImageJ 1.45s software (NIH).

DISCUSSION

According to Lee and Kim (2019), after tofacitinib was intravenously (5-50 mg/kg) and orally (10-100 mg/kg) administered to male Sprague–Dawley rats, the AUCs were dose-dependent at doses higher than 50 mg/kg for both routes of administration. Thus, we selected 10 and 20 mg/kg for use as the intravenous and oral doses of tofacitinib, respectively, in the present study.

Following intravenous administration of tofacitinib, the contribution of gastrointestinal (including the biliary) excretion of unchanged tofacitinib to its CL_{NR} was almost negligible. In fact,

tofacitinib was below the detection limit in GI_{24h} for both control and SIDM rats (data not shown); this may have not been due to the chemical or enzymatic degradation of tofacitinib in the gastric fluids of rats. Tofacitinib was found to be stable at 37°C for a 24-h incubation in different buffer solutions with pH values of 2, 4, 7, 9, and 10 at a tofacitinib concentration of 5 µg/mL. Moreover, after bile duct cannulation in 3 rats, $0.703 \pm 0.303\%$ was the percentage of the tofacitinib intravenous dose (10 mg/kg) excreted in the 24-h bile sample as unchanged drug (Lee and Kim, 2019). The aforementioned data suggest that the CL_{NR} of tofacitinib could represent its metabolic clearance. Therefore, the changes in CL_{NR} of tofacitinib listed in Table 2 could indicate changes in its hepatic metabolism in rats.

Following the intravenous administration of tofacitinib to SIDM rats, the significantly smaller AUC observed could have been due to a significantly faster CL than that found in control rats (Table 2). The faster CL in SIDM rats was mainly due to their significantly faster CL_{NR} than that in control rats. Although the CL_R of tofacitinib was also significantly faster in SIDM rats than that in control rats, its contribution to CL of tofacitinib was minor (6.42% and 7.97% for control and SIDM rats, respectively) (Table 2). Thus, the contribution of the changes in CL_R of tofacitinib to its other pharmacokinetic parameters seemed to be minimal. The higher CL_{NR} of tofacitinib in SIDM rats could have been supported by a significantly higher *in vitro* hepatic CL_{int} (Fig. 4) and faster hepatic blood flow rate (Sato *et al.*, 1991) in SIDM rats than those in control rats. This is because the plasma protein binding of tofacitinib was not high (21.9–23.1%) and was not affected by SIDM; thus, the free fractions of tofacitinib were comparable between the 2 groups as previously mentioned. Tofacitinib is a drug with very close to an intermediate (30–70%) hepatic extraction ratio. This is because the hepatic first-pass effect after absorption into the portal vein was 42.0% in rats (Lee and Kim, 2019). Therefore, the higher hepatic CL_{int} in SIDM rats was mainly due to an increase in the protein expression and/or mRNA level of CYP3A1(23), as that of CYP2C11 decreased in SIDM rats (Kim *et al.*, 2005; Lee *et al.*, 2010). The expression of hepatic microsomal CYP1A2, 2B1/2, 2E1, and 3A23 proteins increased 1.9–3.3 times by SIDM compared to the control, whereas the expression of CYP2C11 decreased to 23–37% of the control level in SIDM rats (Kim *et al.*, 2005). The mRNA levels of the CYP isoforms showed a similar pattern to protein expression.

Following intravenous administration of tofacitinib, its CL_R was estimated from the free (unbound to plasma proteins) fractions of the drug in plasma based on CL_R (Table 2) and the plasma protein binding values of tofacitinib (Table 1); CL_R values were estimated to be 3.33 and 6.15 mL/min/kg for control and SIDM rats, respectively. These values were considerably higher than CL_{CR} (i.e., 2.50 and 1.53 mL/min/kg for control and SIDM rats, respectively) (Table 1). These findings indicate that tofacitinib was mainly secreted from the renal tubules of all rats.

Following oral administration of tofacitinib to SIDM rats, AUC was also significantly smaller than that in control rats (Table 2); thus, the F value of tofacitinib in SIDM rats was smaller (33% decrease) than that in control rats. The intestinal first-pass effect of tofacitinib was 46.1% of the oral dose, but its hepatic first-pass effect after absorption into the portal vein was 42.0% of the intravenous dose; this was equivalent to 23.1% of the oral dose based on the 46.1% for the intestinal first-pass effect in rats (Lee and Kim, 2019). The significantly smaller oral AUC

of tofacitinib in SIDM rats may have been due to an increase in its metabolism in the intestine. Based on the *in vitro* intestinal metabolism of tofacitinib, its K_m values were comparable between control and SIDM rats but V_{max} values were significantly faster in SIDM rats, which resulted in the faster CL_{int} in SIDM rats compared to control rats (Fig. 4). The expressions of CYP isozymes in the intestine were not reported. Our data showed that similar changes of CYP isozymes were found in the intestinal microsomes as well as the hepatic microsomes. Although the expression level of CYP2C11 was minimally decreased, the protein expression level of CYP3A1(23) was markedly increased in the intestine of SIDM rats. The interesting result was that the protein level of P-gp was remarkably increased in the intestine of SIDM rats, indicating that the highly expressed P-gp decreased the absorption of tofacitinib in SIDM rats as tofacitinib is a substrate of P-gp (Hussa, 2014). After oral administration of tofacitinib to SIDM rats, low AUC values were due to decreased absorption and faster metabolism of tofacitinib through the higher expression of P-gp and CYP3A1(23) in the intestine and these resulted in a lower F in SIDM rats than control rats.

The higher concentration and T/P ratios of tofacitinib in different tissues of SIDM rats were reflected in the higher V_{ss} values, which increased by 262% in SIDM rats. The increase in V_{ss} may not be due to the increase in free drug concentration because total protein and albumin in the plasma were unchanged in SIDM rats and the percentage of plasma protein binding of tofacitinib remained unchanged in the 2 groups (Table 1). Therefore, the significant decrease in plasma concentration in SIDM rats was reflected in an increase in the tissue affinity of tofacitinib (Fig. 3). Similar results were also reported for drugs, such as ipriflavone (Lee *et al.*, 2009) and omeprazole (Lee *et al.*, 2007).

Following the intravenous administration of tofacitinib to SIDM rats, its CL_{NR} was found to be significantly higher than that of control rats. This may have been due to the higher hepatic CL_{int} owing to the increase in hepatic CYP3A1(23) and the faster hepatic blood flow rate than those found in the control rats. After tofacitinib was orally administered to SIDM rats, the AUC was significantly smaller than that in control rats. This may have been primarily due to the faster intestinal CL_{int} due to the higher expression of CYP3A1(23) and a decrease in absorption owing to the higher expression of P-gp in the intestine of SIDM rats. These pharmacokinetic changes of tofacitinib in SIDM rats will provide useful information for its clinical application to rheumatoid arthritis patients with diabetes. Further, they will aid in the adjustment of the tofacitinib dosage for these patients.

CONFLICT OF INTEREST

The authors declare no conflicts of interest.

ACKNOWLEDGMENTS

This work was supported by the Korea Health Technology R&D Project (HI16C0992) through the Korea Health Industry Development Institute (KHIDI) funded by the Ministry of Health and Welfare and the Basic Science Research Program (NRF-2018R1A2B6004895) through the National Research Foun-

dition of Korea (NRF) grant funded by the Ministry of Science and ICT (MSIT), Republic of Korea.

REFERENCES

- Antonelli, E., Villanacci, V. and Bassotti, G. (2018) Novel oral-targeted therapies for mucosal healing in ulcerative colitis. *World J. Gastroenterol.* **24**, 5322-5330.
- Bachelez, H., van de Kerkhof, P. C., Strohal, R., Kubanov, A., Valenzuela, F., Lee, J. H., Yakusevich, V., Chimenti, S., Papacharalambous, J., Proulx, J., Gupta, P., Tan, H., Tawadrous, M., Valdez, H. and Wolk, R.; OPT Compare Investigators (2015) Tofacitinib versus etanercept or placebo in moderate-to-severe chronic plaque psoriasis: a phase 3 randomised non-inferiority trial. *Lancet* **386**, 552-561.
- Bae, S. H., Park, J. H., Choi, H. G., Kim, H. and Kim, S. H. (2018) Imidazole antifungal drugs inhibit the cell proliferation and invasion of human breast cancer cells. *Biomol. Ther. (Seoul)* **26**, 494-502.
- Carnovale, C. E., Marinelli, R. A. and Rodriguez Garay, E. A. (1986) Bile flow decrease and altered bile composition in streptozotocin-treated rats. *Biochem. Pharmacol.* **35**, 2625-2628.
- Chiou, W. L. (1978) Critical evaluation of the potential error in pharmacokinetic studies of using the linear trapezoidal rule method for the calculation of the area under the plasma level-time curve. *J. Pharmacokinet. Biopharm.* **6**, 539-546.
- Choi, Y. H., Lee, D. C. and Lee, M. G. (2008) Changes in metformin pharmacokinetics after intravenous and oral administration to rats with short-term and long-term diabetes induced by streptozotocin. *J. Pharm. Sci.* **97**, 5363-5375.
- Claxton, L., Taylor, M., Soonasra, A., Bourret, J. A. and Gerber, R. A. (2018) An economic evaluation of tofacitinib treatment in rheumatoid arthritis after methotrexate or after 1 or 2 TNF inhibitors from a U.S. payer perspective. *J. Manag. Care Spec. Pharm.* **24**, 1010-1017.
- Coombs, J. H., Bloom, B. J. and Breedveld, F. C. (2010) Improved pain, physical functioning and health status in patients with rheumatoid arthritis treated with CP-690,550, an orally active Janus kinase (JAK) inhibitor: results from randomized, double-blind, placebo-controlled trial. *Ann. Rheum. Dis.* **69**, 413-416.
- Dowty, M. E., Lin, J., Ryder, T. F., Wang, W., Walker, G. S., Vaz, A., Chan, G. L., Krishnaswami, S. and Prakash, C. (2014) The pharmacokinetics, metabolism, and clearance mechanisms of tofacitinib, a janus kinase inhibitor, in humans. *Drug Metab. Dispos.* **42**, 759-773.
- Duggleby, R. G. (1995) Analysis of enzyme progress curves by nonlinear regression. *Methods Enzymol.* **249**, 61-90.
- Fukuda, T., Naganuma, M. and Kanai, T. (2019) Current new challenges in the management of ulcerative colitis. *Intest. Res.* **17**, 36-44.
- Gibaldi, M. and Perrier, D. (1982) Pharmacokinetics, 2nd ed. Marcel Dekker, New York.
- Gupta, P., Alvey, C. and Wang, R. (2012) Lack of effect of tofacitinib (CP-690,550) on the pharmacokinetics of the CYP3A4 substrate midazolam in healthy volunteers: confirmation of *in vitro* data. *Br. J. Clin. Pharmacol.* **74**, 109-115.
- Hussa, D. A. (2014) 2013 new drug update: what do new approvals hold for the elderly? *Consult. Pharm.* **29**, 224-238.
- Kennedy Crispin, M., Ko, J. M., Craiglow, B. G., Li, S., Shankar, G., Urban, J. R., Chen, J. C., Cerise, J. E., Jabbari, A., Winge, M. C., Marinovich, M. P., Christiano, A. M., Oro, A. E. and King, B. A. (2016) Safety and efficacy of the JAK inhibitor tofacitinib citrate in patients with alopecia areata. *JCI Insight* **1**, e89776.
- Kim, S. H., Choi, Y. M. and Lee, M. G. (1993) Pharmacokinetics and pharmacodynamics of furosemide in protein-calorie malnutrition. *J. Pharmacokinet. Biopharm.* **21**, 1-17.
- Kim, S. H., Lee, J. S. and Lee, M. G. (1999) Stability, blood partition and plasma protein binding of ipriflavone, an isoflavone derivative. *Biopharm. Drug Dispos.* **20**, 355-360.
- Kim, Y. C., Lee, A. K., Lee, J. H., Lee, I., Lee, D. C., Kim, S. H., Kim, S. G. and Lee, M. G. (2005) Pharmacokinetics of theophylline in diabetes mellitus rat: induction of CYP1A2 and CYP2E1 on 1,3-dimethyluric acid formation. *Eur. J. Pharm. Sci.* **26**, 114-123.
- LaBranchem, T. P., Jesson, M. I., Radi, Z. A., Storer, C. E., Guzova, J. A., Bonar, S. L., Thompson, J. M., Happa, F. A., Stewart, Z. S., Zhan, Y., Bollinger, C. S., Bansal, P. N., Wellen, J. W., Wilkie, D. P., Bailey, S. A., Symanowicz, P. T., Hegen, M., Head, R. D., Kishore, N., Mbalaviele, G. and Meyer, D. M. (2012) JAK inhibition with tofacitinib suppresses arthritic joint structural damage through decreased RANKL production. *Arthritis Rheum.* **64**, 3531-3542.
- Lawendy, N., Krishnaswami, S., Wang, R., Gruben, D., Cannon, C., Swan, S. and Chan, G. (2009) Effect of CP-690,550, an orally active janus kinase inhibitor, on renal function in healthy adult volunteers. *J. Clin. Pharmacol.* **49**, 423-429.
- Lee, D. Y., Chung, H. J., Choi, Y. H., Lee, U., Kim, S. H., Lee, I. and Lee, M. G. (2009) Pharmacokinetics of ipriflavone and its two metabolites, M1 and M5, after the intravenous and oral administration of ipriflavone to rat model of diabetes mellitus induced by streptozotocin. *Eur. J. Pharm. Sci.* **38**, 465-471.
- Lee, J. S. and Kim, S. H. (2019) Dose-dependent pharmacokinetics of tofacitinib in rats: influence of hepatic and intestinal first-pass metabolism. *Pharmaceutics* **11**, e318.
- Lee, D. Y., Lee, M. G., Shin, H. S. and Lee, I. (2007) Changes in omeprazole pharmacokinetics in rats with diabetes induced by alloxan or streptozotocin: faster clearance of omeprazole due to induction of hepatic CYP1A2 and 3A1. *J. Pharm. Pharm. Sci.* **10**, 420-433.
- Lee, J. H., Yang, S. H., Oh, J. M. and Lee, M. G. (2010) Pharmacokinetics of drugs in rats with diabetes mellitus induced by alloxan or streptozotocin: comparison with those in patients with type I diabetes mellitus. *J. Pharm. Pharmacol.* **62**, 1-23.
- Levy, L. L., Urban, J. and King, B. A. (2015) Treatment of recalcitrant atopic dermatitis with the oral Janus kinase inhibitor tofacitinib citrate. *J. Am. Acad. Dermatol.* **73**, 395-399.
- Ma, G., Xie, R., Strober, B., Langley, R., Ito, K., Krishnaswami, S., Wolk, R., Valdez, H., Rottinghaus, S., Tallman, A. and Gupta, R. (2018) Pharmacokinetic characteristics of tofacitinib in adult patients with moderate to severe chronic plaque psoriasis. *Clin. Pharmacol. Drug Dev.* **7**, 584-596.
- Mitruka, B. M. and Rawnley, H. M. (1981) Clinical Biomedical and Hematological Reference Values in Normal Experimental Animals and Normal Humans, 2nd ed. Masson Publishing, USA Inc., New York.
- Molsted, S., Bjørkman, A. S. D., Andersen, M. B. and Ekholm, O. (2018) Diabetes is associated with elevated risks of osteoarthritis, osteoporosis and rheumatoid arthritis. 54th Annual Meeting of the European Association for the Study of Diabetes (EASD). Abstract 1112, Oct. 1-5, 2018, Berlin, Germany.
- Nadai, M., Yoshizumi, H., Kuzuya, T., Hasgawa, T., Johno, I. and Kitazawa, S. K. (1990) Effects of diabetes on disposition and renal handling of cefazolin in rats. *J. Pharmacol. Exp. Ther.* **18**, 565-570.
- Papp, K. A., Menter, M. A., Abe, M., Elewski, B., Feldman, S. R., Gottlieb, A. B., Langley, R., Luger, T., Thaci, D., Buonanno, M., Gupta, P., Proulx, J., Lan, S. and Wolk, R.; OPT Pivotal 1 and OPT Pivotal 2 investigators (2015) Tofacitinib, an oral Janus kinase inhibitor, for the treatment of chronic plaque psoriasis: results from two randomized, placebo-controlled, phase III trials. *Br. J. Dermatol.* **173**, 949-961.
- Park, J. M., Moon, C. H. and Lee, M. G. (1996) Pharmacokinetic changes of methotrexate after intravenous administration to streptozotocin-induced diabetes mellitus rats. *Res. Commun. Mol. Pathol. Pharmacol.* **93**, 343-352.
- Pickup, J. C. and Williams, G. (1991) Textbook of Diabetes. Blackwell Scientific Publications, Oxford.
- Riese, R. J., Krishnaswami, S. and Kremer, J. (2010) Inhibition of JAK kinases in patients with rheumatoid arthritis: scientific rationale and clinical outcomes. *Best Pract. Res. Clin. Rheumatol.* **24**, 5513-5526.
- Sato, H., Terasaki, T., Okumura, K. and Tsuji, A. (1991) Effect of receptor-up-regulation on insulin pharmacokinetics in streptozotocin-treated diabetic rats. *Pharm. Res.* **8**, 563-569.
- Shin, W. G., Lee, M. G., Lee, M. H. and Kim, N. D. (1991) Factors influencing the protein binding of vancomycin. *Biopharm. Drug Dispos.* **12**, 637-646.
- Svein, Ø. and Theodor, W. G. (1982) Comparison of equilibrium time

- in dialysis experiments using spiked plasma or spiked buffer. *J. Pharm. Sci.* **71**, 127-128.
- Tahir, H. (2018) Therapies in ankylosing spondylitis-from clinical trials to clinical practice. *Rheumatology (Oxford)* **57**, vi23-vi28.
- Vincenti, F., Tedesco Silva, H., Busque, S., O'Connell, P., Friedewald, J., Cibrik, D., Budde, K., Yoshida, A., Cohn, S., Weimar, W., Kim, Y. S., Lawendy, N., Lan, S. P., Kudlacz, E., Krishnaswami, S. and Chan, G. (2012) Randomized phase 2b trial of tofacitinib (CP-690,550) in de novo kidney transplant patients: efficacy, renal function and safety at 1 year. *Am. J. Transplant.* **12**, 2446-2456.
- Watkins, J. B., III and Sandeors, R. A. (1995) Diabetes mellitus-induced alterations of hepatobiliary function. *Pharmacol. Rev.* **47**, 1-23.
- Watkins, J. B. III and Sherman, S. E. (1992) Long-term diabetes alters the hepatobiliary clearance of acetaminophen, bilirubin and digoxin. *J. Pharmacol. Exp. Ther.* **260**, 1337-1343.